ADVANCED MATERIALS

In spite of the numerous benefits offered by nanophase materials in general, there are major concerns in the possible use of these materials in the human body due to cytotoxicity.[20] Recently, it has been reported that hepatocyte viability in the presence of CdSe quantum dots[21] and keratinocyte viability in the presence of single-walled carbon nanotubes[22] are adversely affected by the presence of these nanomaterials. In this context, the results from this work, indicating the non-cytotoxic behavior of Si NWs with regard to fibroblast-cell viability, are encouraging and useful for future biomedical applications. Additional in-vitro assays involving orthopedically relevant osteoblast cell lines are in progress.

This work demonstrates the ability of Si NWs to facilitate the growth of uniform, synthetic bone coatings along their surface and to support the facile proliferation of fibroblast cells in their presence. Unlike most biodegradable polymers and ceramics used in orthopedics, nanophase Si in the form of Si NWs is responsive to electrical bias. Therefore, these results set the stage for the fabrication of a broad range of semiconducting Si-based materials of potential value in orthopedics and beyond.

Experimental

Synthesis of Silicon Nanowires (Si NWs): Previously cleaned 1.5 cm × 0.5 cm pieces of low resistivity (0.008–0.02 Ω cm), Sb-doped Si <100> wafers were used as substrates for Si NW synthesis. As an adhesion layer, drops of a 0.1 % (w/v) poly(L-lysine) solution (Ted Pella, Inc.) were first introduced onto the surface and allowed to dry, followed by addition of a layer of 5 nm gold nanocrystals at an approximate concentration of 7.5×10^{12} particles per 1.5 cm × 0.5 cm wafer. This wafer was then placed inside an alumina boat in a custom-built quartz reactor tube equipped with a 6 cm oven. The catalyst was annealed at 600 °C inside the reactor under a He flow (3000 sccm) for ~2 h and then exposed to SiH_4 (0.5 % in He) at a flow rate of 40 sccm for 5 min. A dense network of Si NWs with diameters in the range of 120–180 nm and lengths up to 150 μm was obtained.

Electrochemical Instrumentation: Cathodic-bias experiments were performed in an electrochemical cell where the Si wafer with attached Si NWs was the working electrode, platinum foil was the counter electrode, and simulated body fluid (SBF) solution was the electrolyte. SBF was prepared by mixing 1.37 M NaCl, 0.03 M KCl, 0.042 M $NaHCO_3$, 0.01 M K_2HPO_4, 0.015 M $MgCl_2$, 0.025 M $CaCl_2$, and 0.005 M Na_2SO_4 solutions into a buffer of tris(hydroxymethyl)aminomethane and adjusted with HCl to pH 7.30. A cathodic bias of 1.1 mA cm^{-2} (Keithley Model 236 Source Measure unit) was applied to the Si wafer either for a continuous 3 h period, or alternatively, for a bias for 1 h followed by a 1 week soak in SBF under zero bias. At the end of the experiment, the wafer was rinsed with deionized water and air-dried before characterization.

Cell-Proliferation Experiments: The biocompatibility of Si NWs was studied by monitoring the in-vitro cell-proliferation assays of human kidney fibroblasts in the presence of Si NWs. Human kidney fibroblasts from cell line 293 (American Type Culture Collection) were harvested in Dulbecco's Modified Eagle's Medium (DMEM) containing 10 % fetal bovine serum (FBS). The proliferation of cells was measured by counting the number of cells using a Bright-Line Hemacytometer. The initial cell density was 1.00×10^4 cells mL^{-1}, to which 0.067 mg Si NWs was added. The cells were counted on days 3, 5, and 7 to monitor the proliferation. By day 7, the cell density of fibroblasts had grown to a value of 1.36×10^6 cells mL^{-1}, compared to an average value of 1.15×10^6 cells mL^{-1} for those wells lacking Si NWs (control).

Received: August 20, 2004
Final version: November 22, 2004

[1] Y. Xia, P. Yang, *Adv. Mater.* **2003**, *15*, 353.
[2] Y. Cui, C. M. Lieber, *Science* **2001**, *291*, 891.
[3] Y. Cui, C. M. Lieber, *Science* **2001**, *293*, 1289.
[4] Z. Wang, J. L. Coffer, *Nano Lett.* **2002**, *2*, 1303.
[5] S. H. C. Anderson, H. Elliott, D. J. Wallis, L. T. Canham, J. J. Powell, *Phys. Status Solidi A* **2003**, *197*, 331.
[6] A. P. Bowditch, K. Waters, H. Gale, P. Rice, E. A. M. Scott, *Mater. Res. Soc. Symp. Proc.* **1999**, *536*, 149.
[7] L. T. Canham, *Adv. Mater.* **1995**, *7*, 1033.
[8] D. C. Clupper, J. D. Gough, M. M. Hall, A. G. Clare, W. C. LaCourse, L. L. Hench, *J. Biomed. Mater. Res., Part A* **2003**, *67*, 285.
[9] U. Hersel, C. Dahmen, H. Kessler, *Biomaterials* **2003**, *24*, 4385.
[10] a) L. T. Canham, C. L. Reeves, J. P. Newby, M. R. Houlton, T. I. Cox, J. M. Buriak, M. P. Stewart, *Adv. Mater.* **1999**, *11*, 1505. b) X. Li, J. L. Coffer, Y. Chen, R. F. Pinizzotto, J. Newey, L. T. Canham, *J. Am. Chem. Soc.* **1998**, *120*, 11 706. For reviews, see c) J. M. Buriak, M. P. Stewart, *Adv. Mater.* **2000**, *12*, 859. d) J. M. Buriak, *Chem. Rev.* **2002**, *102*, 1271.
[11] J. Y. Wong, R. Langer, D. E. Ingber, *Proc. Natl. Acad. Sci. USA* **1994**, *91*, 3201.
[12] H. Ozawa, E. Abe, Y. Shibasaki, T. Fukuhara, T. Suda, *J. Cell. Physiol.* **1989**, *138*, 477.
[13] C. E. Schmidt, V. R. Shastri, J. P. Vacanti, R. Langer, *Proc. Natl. Acad. Sci. USA* **1997**, *94*, 8948.
[14] E. De Giglio, L. Sabbatini, P. G. Zambonin, *J. Biomater. Sci., Polymer Ed.* **1999**, *10*, 845.
[15] Y. Cui, C. M. Lieber, *Appl. Phys. Lett.* **2001**, *78*, 2214.
[16] S. Weiner, H. D. Wagner, *Annu. Rev. Mater. Sci.* **1998**. *28*, 271.
[17] C. Loty, J.-M. Sautier, H. Boulekbache, T. Kokubo, H.-M. Kim, N. Forest, *J. Biomed. Mater. Res.* **2000**, *49*, 423.
[18] T. Kokubo, H.-M. Kim, M. Kawashita, *Biomaterials* **2003**, *24*, 2161.
[19] L. T. Canham, C. L. Reeves, D. O. King, P. J. Branfield, J. G. Crabb, M. C. L. Ward, *Adv. Mater.* **1996**, *8*, 850.
[20] V. L. Colvin, *Nat. Biotechnol.* **2003**, *21,* 1166.
[21] A. M. Derfus, W. C. Chan, S. N. Bhatia, *Nano Lett.* **2004**, *4*, 11.
[22] A. A. Shvedova, V. Castranova, E. R. Kisin, D. Schwegler-Berry, A. R. Murray, V. Z. Gandelsman, A. Maynard, P. Baron, *J. Toxicol. Environ. Health, Part A* **2003**, *66*, 1909.

Synthesis of Monodisperse Colloidal Spheres, Capsules, and Microballoons by Emulsion Templating**

By *Carmen I. Zoldesi* and *Arnout Imhof**

The fabrication of hollow-shell particles has been the subject of many recent publications in the field of materials science. These particles play a pivotal role in a wide range of

[*] Dr. A. Imhof, C. I. Zoldesi
Soft Condensed Matter, Debye Institute
Utrecht University
Princetonplein 5, NL-3584 CC Utrecht (The Netherlands)
E-mail: A.Imhof@phys.uu.nl; c.i.zoldesi@phys.uu.nl

[**] This work was supported by the Nederlandse Organisatie voor Wetenschappelijk Onderzoek (NWO). The authors would like to acknowledge J. Meeldijk for assistance with EDX, C. van Kats for the SEM, and A. van Blaaderen for helpful discussions.

  DOI: 10.1002/adma.200401183

industrial and biological applications involving molecular transport, controlled storage and release, adsorption, catalysis, and separation. Potential applications for such particles are as colloidal crystals or highly porous materials. Procedures for the fabrication of hollow spheres have been extensively reported and involve various templating approaches. The templating agents used in the synthesis of hollow particles range from latex,[1–3] silica,[4–7] or gold[8,9] colloidal particles to vesicles.[10–13] The template is subsequently removed by hydrofluoric acid etching (in the case of silica) or by burning in an oven (in the case of latex). The templating technique seems to be an effective route for obtaining hollow spheres from materials as diverse as inorganic ceramics,[1,3,12,14–18] organic polymers,[5–9,11,13,19] and their hybrids.[20] A particularly versatile templating method is the layer-by-layer technique.[1,2] A smaller number of methods employ emulsion-droplet templating to prepare hollow morphologies, which in general lead to polydisperse, hollow particles.[16–18]

We report in this paper on the synthesis and characterization of new types of monodisperse, micrometer-sized, hollow particles obtained by encapsulation of emulsion droplets in solid shells followed by dissolution of the cores. Our method has several important advantages over other techniques. First of all, the liquid cores can be removed under much more benign conditions than solid cores, namely lower temperatures and with "ordinary" solvents like ethanol. Furthermore, by simply tuning the thickness of the shells we can obtain different types of particles, which make them suitable for a variety of applications. Moreover, by using emulsion droplets as templates this technique is conducive to incorporating functional oils or oil-soluble compounds inside the particles. An important advantage of our technique is that we use a facile synthesis method, which leads to monodisperse particles in the micrometer-sized range.

The fabrication scheme for the emulsion-templating approach is as follows: we first prepared monodisperse, stable, oil-in-water emulsion droplets without using surfactant, by hydrolysis and condensation of the difunctional silane monomer dimethyldiethoxysilane (DMDES), following the method described by Vincent and co-workers.[21,22] This led to production of highly monodisperse droplets of low-molecular-weight silicone oil, with diameters in the range 0.6–2 μm. The silicone oil consisted mainly (~90 %) of cyclic octamethylcyclotetrasiloxane, while the remaining compounds were linear –OH-terminated oligomers.[21] We then used the oil droplets as templates for encapsulation by a solid, silica-based shell, which was formed by the hydrolysis and condensation of tetraethoxysilane (TEOS); the liquid cores were easily removed by transferring the particles into ethanol or by evaporation. The synthesis is outlined in detail in the Experimental section. This facile fabrication method allowed us to obtain hollow colloidal particles of diameters in the micrometer-sized range with tunable shell thicknesses and therefore tunable properties, as shown in Figure 1.

The technique we used to prepare the emulsion yielded highly monodisperse oil droplets, by emulsion standards, as shown by the many well-defined minima in the static-light-scattering (SLS) measurements in Figure 2. We obtained the size and polydispersity of the oil droplets by comparing their scattering profiles with theoretical ones calculated using the full Mie solutions for the scattering form factors.[23] The thickness of the coating could be measured

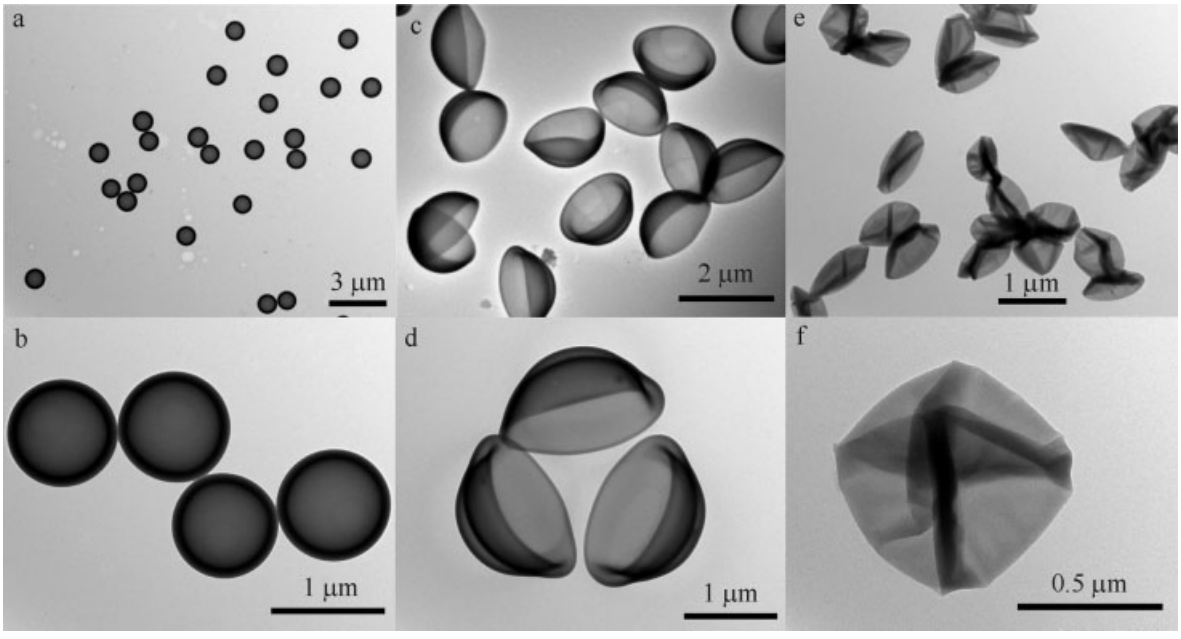

Figure 1. Transmission electron micrographs showing different hollow particles: a,b) hollow microspheres formed by adding TEOS 24 h after DMDES; c,d) microcapsules, TEOS added after 48 h; e,f) microballoons, TEOS added after 72 h.

ADVANCED MATERIALS

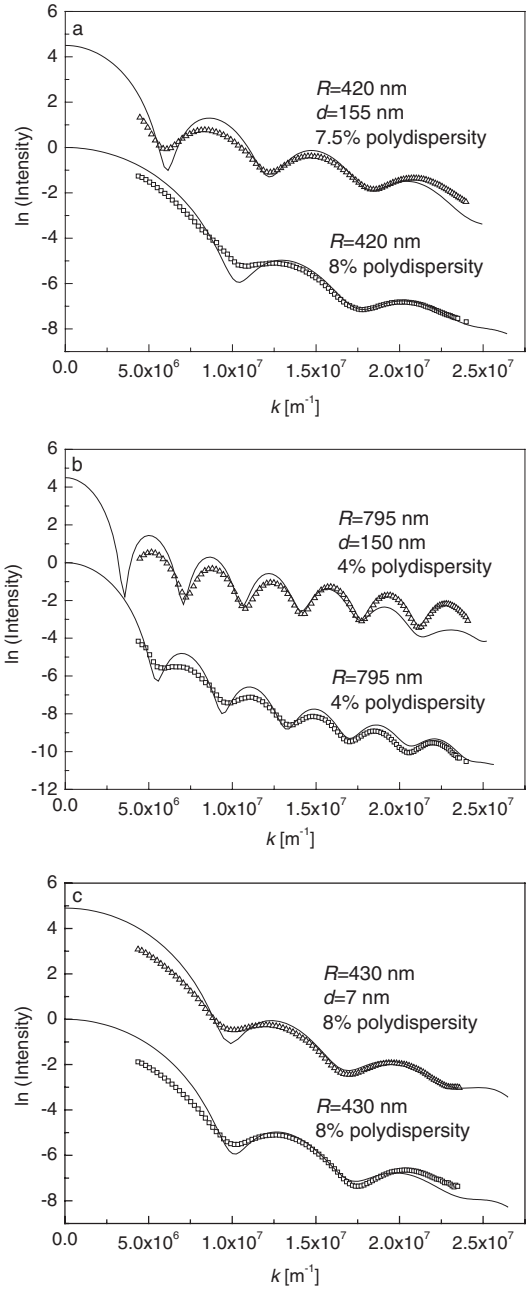

Figure 2. SLS experimental data (scatter points) fitted to theoretical calculations using the full Mie solutions of the form factor (lines): a) squares (bottom) represent data from the oil droplets in water, triangles (top) are data points from the hollow microspheres filled with ethanol obtained from the same oil droplets; b) squares (bottom) are again oil droplets in water and the triangles (top) are the corresponding capsules in ethanol; c) squares (bottom) represent data from the oil droplets in water and triangles (top) are data points from the microballoons in water, still filled with oil. In all plots, *R* represents the core radius and *d*, the shell thickness. We used 1.394 as the refractive index for oil, 1.361 for ethanol, 1.333 for water, and 1.43 for the solid shell (*k* = scattering vector).

from the increase in size after encapsulation using SLS (Fig. 2). Alternatively, transmission electron microscopy (TEM) was used for the same investigations, and its results were in good agreement with those of the SLS analysis. By monitoring the size and polydispersity of the oil droplets over time, we established that the reaction for the formation of the oil droplets at room temperature was relatively slow, with the droplets taking about three days to reach their final size, despite the fact that they were already formed within a few hours. The slow increase in droplet size suggests a slow polymerization of the hydrolyzed monomer and gives us another possibility of choosing the desired size for the templates. Moreover, as we will demonstrate later, the hydrolyzed monomer still present in the emulsion during the encapsulation process contributed significantly to the shell growth and determined the type of particles formed. For a given size of template, the more time elapsed between droplet formation and encapsulation, the thinner was the resulting shell. However, the shell thickness was also influenced by the size of the template; therefore by using different sizes for the templates we could achieve different thicknesses relative to the radii of the templates.

Our approach thus gives us the opportunity to obtain different hollow spheres, of which we distinguish three types. We termed them hollow microspheres (Figs. 1a,b), capsules (Figs. 1c,d), and microballoons (Figs. 1e,f), because their elastic properties apparently depended on the ratio between the shell thickness and the radius of the template. The different possibilities for applications can be derived from their properties. The different spheres were formed when the time between addition of DMDES and TEOS was ~24 h, ~48 h, and ~72 h, respectively. We found that increasing the temperature at which droplet formation took place to 50 °C sped up this sequence to within a period of about 40 h.

The hollow microspheres were characterized by thick, solid shells (from ~20 nm up to 200 nm). A major contribution to the shell thickness was made by the hydrolyzed monomer still present in the emulsion during the encapsulation step. As a result, the shell represented a crosslinked, porous network. Yet, the shells were sufficiently permeable to allow dissolution of the oil after suspending the encapsulated droplets in ethanol. The TEM images (Figs. 1a,b) reveal the hollow structure of the particles. The light-scattering characterization of the samples confirmed the spherical, hollow structure, with the hollow shells being filled with solvent in solution (Fig. 2a).

Because of their high uniformity in size, these particles formed colloidal crystals after sedimenting slowly to the bottom of their container, giving rise to bright Bragg reflections. Figure 3 shows scanning electron microscopy (SEM) images of ordered, hollow spheres. Because of their ability to form ordered structures, we are interested in these particles as precursors for crystals of hollow spheres and also as doping agents in crystals of regular silica particles.

The elemental composition of the hollow microspheres was obtained from energy dispersive X-ray (EDX) investigations. By performing EDX microanalysis in scanning TEM (STEM) mode, the hollow structure of the microspheres, as well as the composition of the shell (which was rich in carbon because of the monomer contribution, see Fig. 4a) was revealed. The

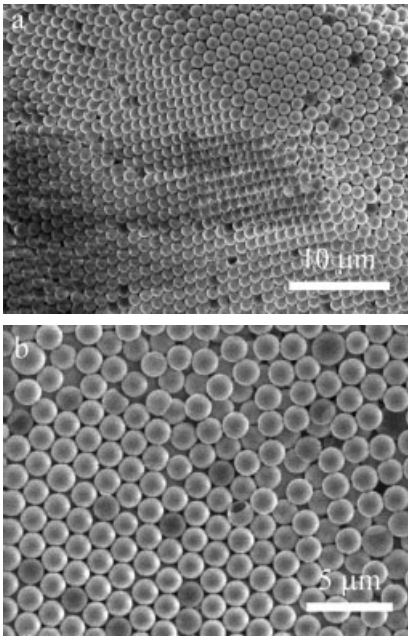

Figure 3. SEM micrographs of a crystal of hollow microspheres formed by drying a drop of microsphere suspension on a glass slide.

strength of the shells allowed them to sustain calcination at high temperatures (500 °C). As a result, their structure was maintained while a change in composition occurred: the carbon was replaced by oxygen during the calcination in air as shown in Figure 4c. This demonstrates that the shell material was a mixed organic–inorganic copolymer of DMDES and TEOS. The particle size was reduced by 10–12 % as a result of the removal of the organic components.

For capsule-like particles (Figs. 1c,d) the amount of hydrolyzed monomer which contributed to the shell thickness was less than for the microspheres. As a result, the shells became slightly thinner, more flexible, and surprisingly deformable. In solution, these particles maintained their spherical shape (as demonstrated by the sharp SLS minima, which corresponds to spherical particles, see Fig. 2b), while after drying they collapsed, forming hemispherical caps. Since a pure silica shell would be expected to crack, the high flexibility probably resulted from the large amount of dimethylsiloxane groups in the shell material. Because of their high monodispersity, these particles were also able to form highly ordered structures in solution.

The third category of hollow particles consists of microballoons (Figs. 1e,f). They were characterized by extremely thin shells only a few nanometers in diameter as measured by SLS (Fig. 2c), and could be obtained by encapsulating oil droplets in their final growth stage. The shells were still flexible but apparently much less elastic than the capsules. The different behavior of the capsules and microballoons after drying can be observed in Figure 1, which reveals the difference in the shell elasticity between these two types of particles: while capsules deformed elastically like a rubber ball, the microballoons did not show such a deformation. They exhibited creases and folds due to the collapse of the thin, spherical shells. When packed and dried, the microballoons formed highly porous materials with a large volume of voids.

Our results indicate that emulsion templating can be successfully used to prepare monodisperse, micrometer-sized, hollow particles. We developed a flexible method which allowed us to obtain different types of particles with tunable properties. The resulting particles may have various applications, from making photonic crystals to small containers and porous materials. We are presently investigating the possibility of refilling these particles with liquids and using them as microreactors.

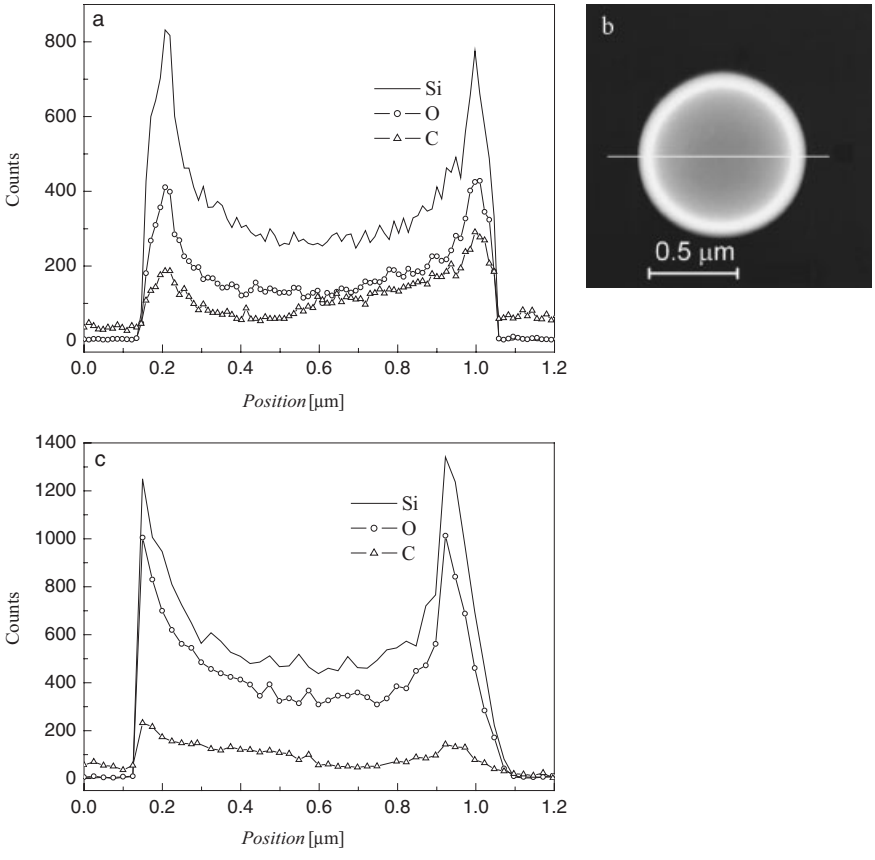

Figure 4. a) EDX line graph obtained in STEM mode by performing the scan indicated in (b). b) TEM dark-field image showing the EDX line-scan through the microsphere (white line; the scan was performed from left to right). c) EDX line graph acquired for a microsphere after calcination in air at 500 °C for 4 h. The carbon signal has a non-zero baseline because we used carbon-coated TEM grids.

ADVANCED MATERIALS

Experimental

Low-molecular-weight polydimethylsiloxane (PDMS) silicone oil-in-water emulsion droplets were synthesized by the base-catalyzed hydrolysis and polymerization of dimethyldiethoxysilane (DMDES, ≥97.0 %, Fluka), in accordance with previously done work [21]. The continuous phase of the emulsions was prepared by adding between 1 and 25 vol.-% ammonia (29.7 wt.-% NH_3; Merck) to de-mineralized water. Different volume fractions of monomer, in the range 0.01 to 0.04, were then added to the aqueous solutions and vigorously shaken for a few minutes. The emulsion droplets already formed within a few hours, but they were allowed to grow for at least 24 h before being coated.

The encapsulation of the oil droplets with a solid shell was achieved by adding 0.018 M tetraethoxysilane (TEOS, ≥99.0 %; Fluka) to the emulsions during stirring. We started the coating after 24, 48, or 72 h, depending on whether we wanted to obtain microspheres, capsules, or microballoons, respectively. The particles were allowed to complete their shell growth for three days. In order to remove the oil from the core, the particles were centrifuged and re-suspended in ethanol, which penetrated the shells and dissolved the oil.

Static light scattering was performed with home-built equipment using a He–Ne laser as a light source (632.8 nm, 10 mW). The angular distribution of the scattered light was measured at scattering angles from 19° to 135° relative to the transmitted beam using a photomultiplier tube mounted on a turntable goniometer. The data were plotted against the scattering vector $k = 4\pi n \sin(\theta/2)/\lambda$, where n is the solvent refractive index, θ is the scattering angle, and λ the wavelength in vacuum. Theoretical form factors were calculated using the full Mie solution for core–shell spheres and fitted to the experimental data, providing the radius and polydispersity [23]. We found good agreement by taking $n(\text{core}) = 1.394$ for the oil droplets in water and $n(\text{core}) = 1.361$ for the ethanol-filled hollow spheres.

TEM images were acquired using a Philips Tecnai 12 transmission electron microscope with an accelerating voltage of 120 keV. The samples were prepared by dipping copper 300 mesh-carrier grids, covered with carbon-coated Formvar films, into dilute suspensions. SEM images were obtained with a Philips XL 30 FEG scanning electron microscope and the samples were prepared by drying a drop of particle suspension on a glass slide.

The EDX measurements were carried out on a Philips Tecnai 20F transmission electron microscope. The accelerating voltage was 200 keV. The same types of samples were used as for the TEM.

Received: July 23, 2004
Final version: November 4, 2004
Published online: February 10, 2005

[1] F. Caruso, R. A. Caruso, H. Mohwald, *Science* **1998**, *282*, 1111.
[2] F. Caruso, *Adv. Mater.* **2001**, *13*, 11.
[3] A. Imhof, *Langmuir* **2001**, *17*, 3579.
[4] C. Graf, A. van Blaaderen, *Langmuir* **2002**, *18*, 524.
[5] L. Zha, Y. Zhang, W. Yang, S. Fu, *Adv. Mater.* **2002**, *14*, 1090.
[6] T. K. Mandal, M. S. Fleming, D. R. Walt, *Chem. Mater.* **2000**, *12*, 3481.
[7] X. Xu, S. A. Asher, *J. Am. Chem. Soc.* **2004**, *126*, 7940.
[8] S. M. Marinakos, D. A. Shultz, D. L. Feldheim, *Adv. Mater.* **1999**, *11*, 34.
[9] K. Kamata, Y. Lu, Y. Xia, *J. Am. Chem. Soc.* **2003**, *125*, 2384.
[10] D. H. W. Hubert, M. Jung, P. M. Frederik, P. H. H. Bomans, J. Meuldijk, A. L. German, *Adv. Mater.* **2000**, *12*, 1286.
[11] C. A. McKelvey, E. W. Kaler, J. A. Zasadzinski, B. Coldren, H.-T. Jung, *Langmuir* **2000**, *16*, 8285.
[12] H.-P. Hentze, S. R. Raghavan, C. A. McKelvey, E. W. Kaler, *Langmuir* **2003**, *19*, 1069.
[13] M. Sauer, D. Streich, W. Meier, *Adv. Mater.* **2001**, *13*, 1649.
[14] J. J. L. M. Cornelissen, E. F. Connor, H.-C. Kim, V. Y. Lee, T. Magibitang, P. M. Rice, W. Volksen, L. K. Sundberg, R. D. Miller, *Chem. Commun.* **2003**, 1010.
[15] Y. Yin, Y. Lu, B. Gates, Y. Xia, *Chem. Mater.* **2001**, *13*, 1146.
[16] Q. Sun, P. J. Kooyman, J. G. Grossmann, P. H. H. Bomans, P. M. Frederik, P. C. M. M. Magusin, T. P. M. Beelen, R. A. van Santen, N. A. J. M. Sommerdijk, *Adv. Mater.* **2003**, *15*, 1097.
[17] M. Jafelicci, Jr., M. R. Davolos, F. J. dos Santos, S. J. de Andrade, *J. Non-Cryst. Solids* **1999**, *247*, 98.
[18] J.-H. Park, C. Oh, S.-I. Shin, S.-K. Moon, S.-G. Oh, *J. Colloid Interface Sci.* **2003**, *266*, 107.
[19] S. Liu, D. F. O'Brien, *J. Am. Chem. Soc.* **2002**, *124*, 6037.
[20] O. Emmerich, N. Hugenberg, M. Schmidt, S. S. Sheiko, F. Baumann, B. Deubzer, J. Weis, J. Ebenhoch, *Adv. Mater.* **1999**, *11*, 1299.
[21] T. M. Obey, B. Vincent, *J. Colloid Interface Sci.* **1994**, *163*, 454.
[22] M. I. Goller, T. M. Obey, D. O. H. Teare, B. Vincent, M. R. Wegener, *Colloids Surf. A* **1997**, *123*, 183.
[23] C. F. Bohren, D. R. Huffman, *Absorption and Scattering of Light by Small Particles*, John Wiley and Sons, New York **1983**.

Fabrication of Ruthenium–Carbon Nanotube Nanocomposites in Supercritical Water**

By *Zhenyu Sun*, *Zhimin Liu*,* *Buxing Han*,* *Yong Wang*, *Jimin Du*, *Zailai Xie*, *Guojun Han*

Carbon nanotubes (CNTs) have stimulated intensive interest in the past decade owing to their exceptional electrical[1] and mechanical[2] properties, and they have a variety of potential applications, including field-effect transistors,[3] full-color displays,[4] chemical actuators,[5] tips for scanning-probe microscopes,[6] molecular computers,[7] and hydrogen storage.[8] It is worth pointing out that CNTs are currently being considered as new supports for metal and semiconductor catalysts because of their small size, high chemical stability, and large surface area. Many catalytic metal nanoparticles have been decorated on CNTs,[9–17] including ruthenium (Ru), which plays an important role in the chemical industry. It has been shown previously that Ru is one of the best catalysts for Fischer–Tropsch synthesis,[18] water–gas shift reaction,[19] ammonia synthesis,[20,21] hydrogenation of benzene,[22] hydrogenolysis,[23] higher alcohol synthesis,[24] and the Kobel–Engelhardt reaction.[25] Nanometer-sized Ru particles with a high density of active sites usually exhibit favorable catalytic properties.

[*] Dr. Z. M. Liu, Prof. B. X. Han, Z. Y. Sun, Y. Wang, J. M. Du, Z. L. Xie, G. J. Han
Center for Molecular Sciences, Institute of Chemistry
Chinese Academy of Sciences
Beijing 100080 (P.R. China)
E-mail: liuzm@iccas.ac.cn, hanbx@iccas.ac.cn

[**] This work is financially supported by the National Natural Science Foundation of China (nos. 50472096, 20133030).

  DOI: 10.1002/adma.200400839